

Size-induced effects in gallium selenide electronic structure: The influence of interlayer interactions

D. V. Rybkovskiy,^{1,2,*} N. R. Arutyunyan,¹ A. S. Orekhov,^{1,3} I. A. Gromchenko,^{1,4} I. V. Vorobiev,¹ A. V. Osadchy,¹
E. Yu. Salaev,⁵ T. K. Baykara,⁶ K. R. Allakhverdiev,^{5,6} and E. D. Obraztsova¹

¹*A.M. Prokhorov General Physics Institute, Russian Academy of Sciences, Vavilova 38, Moscow 119991, Russia*

²*Moscow State Institute of Radiotechnics, Electronics and Automation (Technical University), Prospect Vernadskogo 78, Moscow 119454, Russia*

³*The Shubnikov Institute of Crystallography, Russian Academy of Sciences, Leninskii prospekt 59, Moscow 119333, Russia*

⁴*M.V. Lomonosov Moscow State University, Vorobevy Gory 1, Moscow 119992, Russia*

⁵*Institute of Physics ANAS, Baku, Azerbaijan 370073*

⁶*Institute of Materials Science, TUBITAK, Gebze, Koçaeli, Turkey P. K. 21, 41470*

(Received 11 March 2011; revised manuscript received 28 July 2011; published 25 August 2011)

The electronic structure of two-dimensional gallium selenide crystals containing a small number of layers was investigated theoretically and experimentally. The electronic band structure of the layered GaSe crystal was investigated by the first-principles density functional theory calculations. The *GW* approximation was used for the correction of the band-gap values. A dependence of the band-gap value on the number of tetralayers has been demonstrated. For the thin crystal with several tetralayers, the band gap becomes larger compared to the bulk crystal. The thin layers of GaSe have been experimentally produced by the ultrasonication of GaSe particles in water suspensions in the presence of Pluronic F127 surfactant. Their thickness was from one to a few tetralayers, according to the transmission electron microscopy studies. The optical absorption spectra demonstrate the well-resolved bands, shifted toward the blue relative to those of the bulk GaSe. Their origin is caused by the presence of GaSe structures with one to a few tetralayers.

DOI: [10.1103/PhysRevB.84.085314](https://doi.org/10.1103/PhysRevB.84.085314)

PACS number(s): 31.15.A–, 73.22.–f, 81.07.St

I. INTRODUCTION

Gallium selenide is a layered chalcogenide semiconductor crystal. Depending on the layer stacking and their numbers in the unit cell, GaSe crystallizes in four different polytypes.^{1,2} Each layer of GaSe consists of four monoatomic sheets of Se-Ga-Ga-Se atoms (Fig. 1). Inside such tetralayers, Ga and Se atoms are bonded covalently. The tetralayers are connected predominantly by van der Waals forces, so the interlayer coupling is relatively weak.

The electronic properties of bulk GaSe crystals were investigated with various techniques. The first calculations of the electronic band structure of this material were performed within the two-dimensional (2D) tight-binding (TB) approach,^{3,4} neglecting the interlayer interactions. The TB band structures of GaSe in 2D⁵ and 3D^{6,7} have also been calculated, including the effects of Se-Se interactions along the optical *c* axis.

Schlüter^{8,9} and other groups¹⁰ have carried out more accurate calculations for β -GaSe using the empirical pseudopotential method.⁸ These results have provided important information for understanding the optical properties of this material. Several investigations were based on the improved TB formalism,¹¹ density functional theory (DFT),^{12,13} and augmented plane waves, plus the local orbital¹⁴ methods.

To the best of our knowledge, up to now there are no results published on the electronic structure of thin GaSe crystals with a small number of layers. At the same time, the reduced dimensionality can lead to significant changes of the electronic properties of materials. In 2D systems, known as quantum wells, the band-gap value is controlled by the system thickness. In the case of layered compounds, such control can be carried out by varying the number of layers. Due to a weak interlayer coupling, this approach can be technologically

preferable. Some structures with few layers have already been theoretically studied (graphite and graphene¹⁵). These investigations have shown that the electronic structure of a single layer should be different from that of the bulk material due to the absence of interlayer interactions.

The attempt to observe the size-induced effects in GaSe was made by a few groups. In order to obtain GaSe nanoparticles, the methods of metalorganic chemical vapor deposition (MOCVD)¹⁶ (Ga₄Se₄R₄ cubanes were used as a source) and GaSe sonication in methanol were proposed.¹⁷ It was reported¹⁷ that the optical absorption spectra of crystallites with a diameter of ≤ 20 nm turned out to be blueshifted. No control of the obtained particle size could be guaranteed, and no reproducible observation of the size-induced quantum effects has been made. The gallium selenide nano-disks of a smaller diameter (2–10 nm) have been synthesized successfully in 2002.¹⁸ GaSe synthesis is based on the reaction of an organometallic (GaMe₃) with a trioctyl phosphine selenium in a high-temperature solution of trioctyl phosphine and trioctyl phosphine oxide. The resulting nanoparticles were formed as single tetralayers due to the weak van der Waals forces between the layers and also the interactions with the solvent.

The shoulder arising in the optical absorption spectrum due to the GaSe nanoparticles^{18–21} was situated at ~ 400 nm depending on the particle size. The position of this shoulder was strongly shifted to higher energies comparing with that of the bulk GaSe crystals. The emission spectra^{18–21} were shifted to higher energies too, with the maximum of emission positioned at ~ 400 –450 nm. The authors explained the blueshift of photoluminescence and optical absorption as an action of a 3D size-induced effect. The present research was focused on the investigation of the size-induced effects caused by the 1D reduction of GaSe thickness. The dependence of a

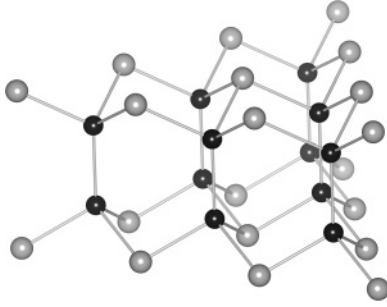


FIG. 1. The crystal structure of a single GaSe tetralayer. The dark and bright spheres represent Ga and Se atoms, respectively.

GaSe electronic structure on the number of layers has been analyzed in experimental and theoretical studies.

II. THEORETICAL ELECTRONIC BAND STRUCTURE

A. DFT calculations

The DFT with a plane-wave basis set was used to calculate the structural parameters and electronic bands of GaSe structures. All calculations were carried out using the ABINIT code.^{22,23} The Trouiller-Martins pseudopotentials were employed. To describe the exchange and correlation, the local density approximation (LDA) was applied. The 4s and 4p electrons of Ga and Se were treated as the valence electrons. In the case of 2D GaSe structures, 13 k points for the first Brillouin zone integration and a cutoff energy of 20 Hartree was used. The computations of the bulk material were performed with 68 k points and a cutoff of 30 Ha. In multilayered structures, the layers were stacked together according to the ϵ polytype (space group $D3h1$, contains two layers per unit cell¹).

Starting with the structural parameters close to the experimental data, we performed a geometrical optimization of the ϵ -GaSe crystal. The results of this procedure are shown in Table I. There are no experimental results published for the systems with a small number of tetralayers. For the bulk material, the computation gives the smaller lattice constants compared to the experimental data. This discrepancy can be caused by the exclusion of Ga 3d electrons from our computations. The difference of the lattice constants between the bulk GaSe and a single tetralayer is less than 0.01 Å. It should be mentioned that the GaSe crystal is a complicated system for the structural optimization procedure, since it includes the interlayer van der Waals interactions not taken into account within the DFT. The use of LDA usually leads to the underestimation of the interatomic distances and the lattice constants, while the GGA overestimates them.

After the structural optimization, the electronic dispersions have been calculated. Though in the case of a 2D system the dispersion along Γ -A has no physical meaning, the curves were plotted along the high-symmetry directions of a 3D Brillouin zone, so that the electronic structures of thin and bulk crystals could be directly compared. The resulting band structure for a single GaSe tetralayer is shown in Fig. 2. The zero for the energy is adjusted to the valence-band maximum. An absence of dispersion along the A- Γ direction and the

TABLE I. The lattice constants of GaSe structures obtained from DFT calculations. The experimental values for bulk GaSe are taken from Refs. 7 and 24.

	a (Å)	c (Å)
Bulk GaSe [experiment (Ref. 7)]	3.73	15.9
Bulk GaSe [experiment (Ref. 24)]	3.743	15.919
Bulk GaSe	3.662	15.587
One tetralayer	3.657	—
Two tetralayers	3.658	—
Three tetralayers	3.658	—
Four tetralayers	3.659	—

identification of the band structures in the Γ - M - K and A - L - H planes indicates a 2D character of the single GaSe tetralayer. Unlike the bulk material, the valence-zone maximum is not located at the Γ point, but it is shifted to the K and M points. Thus, the corresponding dispersion curve at Γ has a local minimum. The highest occupied energy band is formed by p_z orbitals of the selenium atoms and s orbitals of the gallium atoms. Four lower bands, which are double degenerated at Γ , are formed by p_x and p_y orbitals of selenium atoms. Their closeness is caused by a weak intralayer π -type interaction. The bottom of the conduction zone is located at the M point.

The addition of the second tetralayer leads to a splitting of the energy bands due to the interlayer interactions (Fig. 3). The states of the valence zone top are significantly split due to a strong overlap of the selenium p_z orbitals of the neighboring layers. It leads to a change of the band-gap value, because these states are the topmost valence bands. The p_x and p_y orbitals of the neighboring layers interact very weakly, and this leads to a small splitting of the corresponding bands. The maxima

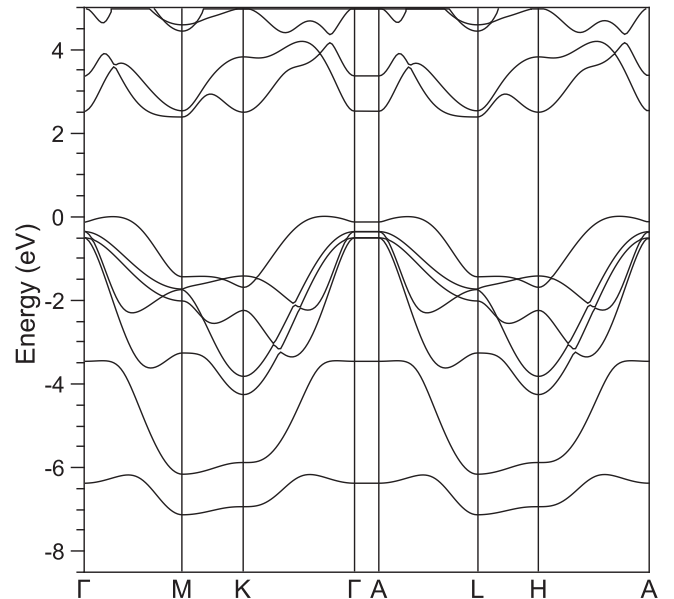


FIG. 2. The electronic band structure of a single GaSe tetralayer, calculated using a DFT-LDA method. The zero of the energy scale is adjusted to the valence-band maximum. The lowest two Se s bands are not shown.

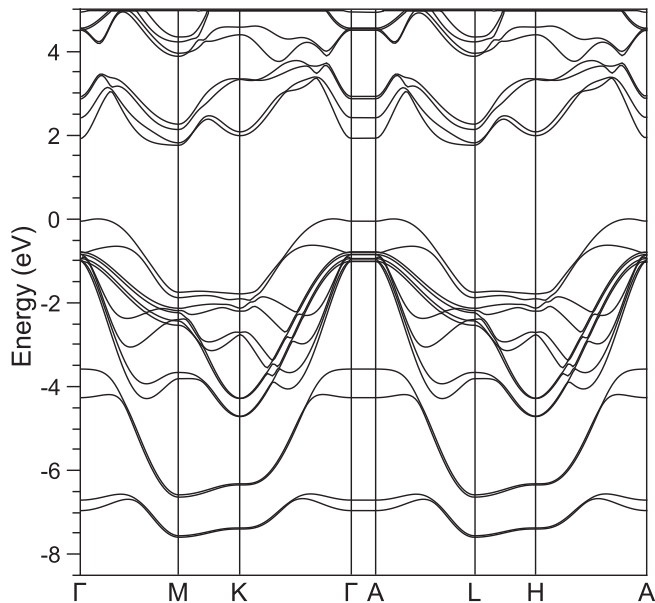


FIG. 3. The electronic band structure of two GaSe tetralayers, calculated using a DFT-LDA method. The zero of the energy scale is adjusted to the valence-band maximum. The lowest four Se s bands are not shown.

of the valence zone are shifted to the Γ point compared with those of a single tetralayer structure. Further increasing of the system thickness by adding an additional tetralayer leads to a further splitting of the energy bands and to a shifting of the top valence band to the Γ point. This causes the narrowing of the band gap.

When there are many layers included, the electronic structure becomes similar to that of the bulk gallium selenide (Fig. 4). In this case the topmost valence band is located at Γ and the lowest conduction band is located at M , which is in an agreement with the experimental results and previous calculations.⁹ Since the unit cell of bulk ε -GaSe extends over two layers, the number of energy bands is equal to that of the two tetralayer structure. The dispersion along the Γ - A direction can be a rough measure of the strength of the interlayer interactions. In the A - L - H plane the band structure is similar to the single GaSe tetralayer, while in the Γ - M - K plane the bands of the bulk material are split due to the interlayer interactions.

B. GW approximation and correction of the band-gap values

It is well known that DFT underestimates the conduction-band energies. At the same time, for a correct description of the quantum confinement effect, correct quantitative results for the band-gap values have to be obtained. To our knowledge there are no theoretical first-principles calculations performed for single tetralayer systems of GaSe. The only available result was obtained within the effective-mass approach based on the electron and hole effective masses of bulk GaSe.²⁵ Unfortunately this method fails to describe quantitatively the quantum confinement along the z direction.

To adjust the DFT band-gap values, we have performed calculations in frames of GW approximation^{26,27} for systems

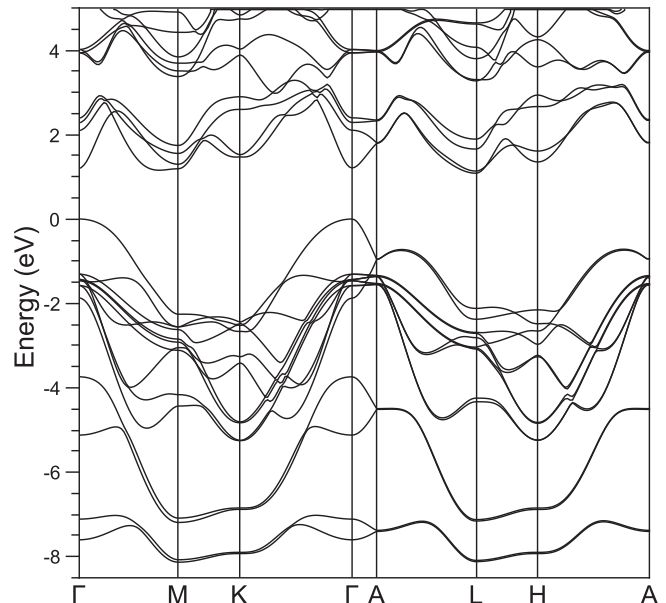


FIG. 4. The electronic band structure of bulk GaSe, calculated using a DFT-LDA method. The zero of the energy scale is adjusted to the valence-band maximum. The lowest four Se s bands are not shown.

with several tetralayers and for the bulk material. We made the GW corrections only for the center of the Brillouin zone. The integration over the frequency in the self-energy was carried out by the plasmon-pole model.

The Kohn-Sham data, obtained by performing DFT calculations, was the starting point of our GW computations. On this basis, the dielectric matrix and its inverse were calculated. Then the Kohn-Sham band structure and the screened interaction were used to evaluate the matrix elements of the self-energy operator.

The values of the computation parameters used in our investigations are shown in Table II. The resulting band gaps at the center of the Brillouin zone are plotted in Fig. 5. The obtained value of the direct band gap for the bulk GaSe ($E_g = 2.34$ eV) is slightly larger than the experimental value 2.12 eV,^{28,29} but it is much better than the LDA estimation result ($E_g = 1.21$ eV). Such disparity between the theoretical and experimental values may appear due to the neglect of Ga $3d$ electrons. For a single tetralayer, the GW band gap at Γ is equal to 3.89 eV. Another important point is that the electronic structure of GaSe strongly depends on the interatomic distances. For example, similar calculations, performed for gallium selenide with the nonrelaxed experimental lattice constants and interatomic distances (Ref. 24), give the band-gap values equal to 1.99 and 3.57 eV for a bulk material and for a single tetralayer, respectively. At the same time, the experimental values of the crystal geometry vary in a wide range (Refs. 2,7,24). Thus, an accurate quantitative determination of the band gap for thin GaSe systems is a difficult task. However, qualitatively, the quantum confinement effect, induced by the reduction of the crystal thickness, and the dependence of the band-gap values on the number of tetralayers can be clearly seen from our calculations.

TABLE II. The convergence parameters for the *GW* calculations.

	Calculation of the screening			Calculation of the self-energy matrix elements		
	Number of bands	Energy cutoff (Ha)		Number of bands	Energy cutoff (Ha)	
		Wave function	Dielectric matrix		Wave function	Exchange part of the self-energy
1 layer	100	8	4	150	7	10
2 layers	100	8	4	250	8	8
3 layers	350	6	7	350	8	9
4 layers	450	8	4	450	8	9
Bulk	350	9	5	300	6	5

III. EXPERIMENTAL ANALYSIS OF GaSe LAYERS

A. Fabrication of thin GaSe platelets

The initial GaSe (predominantly ϵ polytype) crystals were grown by the Bridgman-Stockbarger method and ground into powder with the particle size down to 20 μm . The further reduction of GaSe particle size was achieved by the ultrasonication of the GaSe suspensions followed by the microfiltration. The sonication of GaSe crystals leads to the bond break, especially the weak ones between the tetralayers. The particles agglomerate quickly (1 h) and form large GaSe clusters. In this paper, it is proposed to use the surfactants to prevent the aggregation and to isolate the GaSe particles from each other and from the solvent (water in this case). Pluronic F127 was used as the surfactant. Its typical concentration was 1 wt %.

The GaSe macrocrystals were added to the Pluronic F127/H₂O solution. The concentration of the GaSe crystals was 0.1 mg/ml. A relatively low concentration has been chosen to avoid the aggregation of GaSe particles. The suspension was treated by the ultrasonic Hielscher UP200 (power 450 W) for 1 h. The resulting brown-colored suspension was labeled as sample A. This suspension was left for the sedimentation; the large particles went down. The upper part was then taken and sonicated for 1 h more. Then the suspension was filtered through the nitrocellulose microfilters (Millipore, pore size 200 nm). The fraction that went through the filter contained

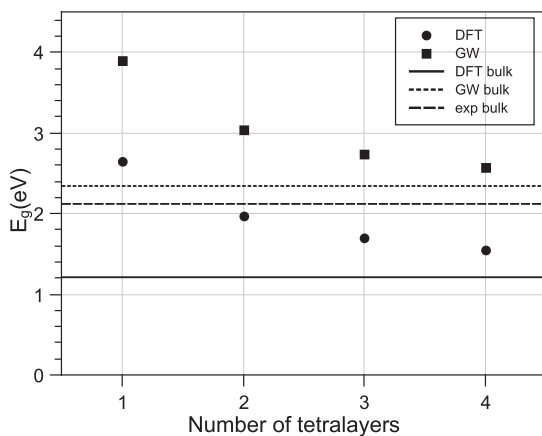


FIG. 5. The variation of the band gap depending on the number of GaSe tetralayers. The lines represent the bulk band gaps.

mostly the particles smaller than 200 nm. The suspension was stable in time for at least 150 h. It was controlled by the optical absorption spectroscopy. This orange-colored fraction was labeled as sample B. After more than 150 h, the particles of GaSe tended to the sedimentation and to the aggregation. In this situation a repetition of the sonication and filtration was applied to achieve the suspension with the initial size distribution.

B. Transmission electron microscopy

The structural transmission electron microscopy (TEM) study was carried out by a conventional bright- and dark-field transmission microscopy (BF/DF-TEM), electron microdiffraction using FEI Tecnai G2 30 S-TWIN. A microscope was supplied with an x-ray energy-dispersive microanalysis EDX. Images were recorded on the Gatan 797 slow scan CCD camera and processed with the Gatan Digital Micrograph software. Phase identification was performed by analyzing the selected area electron-diffraction patterns (SAED) taken on micrometer-scale areas. For this purpose, the diffraction patterns were calculated using the Java Electron Microscopy Software (JEMS) for electron-optical parameters of the microscope given above and the structural data of gallium selenide. The GaSe suspension was deposited on a copper grid with a holey amorphous carbon film and dried under air conditioning.

A TEM image of sample A (Fig. 6) shows that it consists of the small and large (up to 4–5 μm in size) flat crystals. All crystals have well-defined edges. Some of the crystals are flat thin platelets, but most are thick enough to be treated as a bulk GaSe. An electron diffraction pattern from one of the crystal blocks is shown in the inset of Fig. 6. This pattern was identified as a [001] zone axis hexagonal structure with $a = 3.75 \text{ \AA}$ and $c = 15.92 \text{ \AA}$ lattice parameters which correspond to gallium selenide (space group $P63/mmc$).¹

On the contrary, sample B consists of small flat nonisometric gallium selenide crystals. Figure 7 shows the TEM image of the agglomeration of gallium selenide crystals. A low contrast of crystals means that after ultrasonic destruction the gallium selenide crystals were thin. An analysis of the image contrast reveals that the agglomeration consists of an array of large and small ($\sim 50 \text{ nm}$) flat blocks attached to the particle lying above the carbon film hole.

Among large arrays of gallium selenide block crystals, small isometric particles $\sim 15 \text{ nm}$ in diameter were found. Figure 8 (left-hand side) shows a BF-TEM image of these

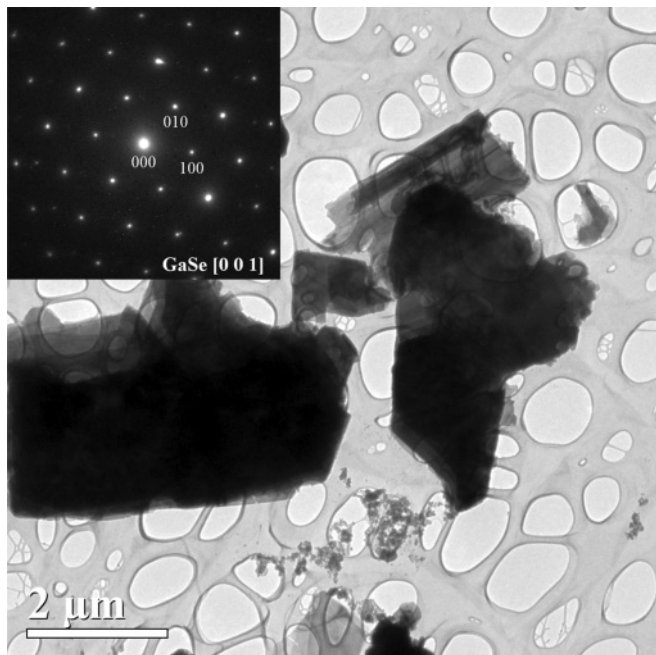


FIG. 6. TEM image of nonfiltered GaSe sample (type A). The inset shows the selected area electron-diffraction pattern of a hexagonal GaSe crystal.

particles with a round shape. A DF-TEM was done in order to prove that these particles are GaSe. Figure 8 (right-hand side) shows a DF image obtained in the 010 GaSe reflex zone axis [001].

C. Optical-absorption spectroscopy

The optical-absorption spectra were registered with a 1-nm spectral resolution (Spectrophotometer Perkin Elmer Lambda-950) in a 1-cm-thick quartz cell. The optical-absorption spectra of GaSe particles have been registered for two types of samples: A and B. The A samples were the suspensions contained large GaSe crystals (most of a particle size > 500 nm). Type A was used as a reference in order to estimate the influence of the particle size and the thickness on the band-gap value. The B samples were the suspensions of small GaSe crystals (< 200 nm), prepared as described in Sec. III A.

The optical-absorption spectra of samples A and B are presented in Fig. 9. The large thick particles of GaSe (sample A) have the typical absorption band at 620 nm. Its position corresponds to the absorption band of the indirect excitons in a macroscopic GaSe crystal.^{1,17} The weak line at 415 nm can be observed as well. However, its relative intensity is much lower compared with the 620-nm line, which is attributed to the bulk volume GaSe.

The spectrum of sample B is shifted to the blue region. The main absorption bands are situated at 560, 415, and 340 nm. After sedimentation and filtering of sample A, the amount of the bulk large particles decreases substantially. Simultaneously, the UV bands are sharpened and intensity increases. The 620-nm band moves toward “blue” and widens. Its relative intensity decreases strongly.

We assume that these transformations of the optical-absorption bands are caused mostly by a change of the

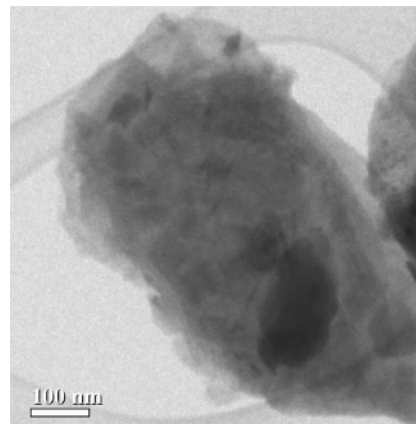


FIG. 7. A BF-TEM image of the thin gallium selenide crystals (sample B).

thickness of GaSe particles. As is discussed in the theoretical part, the band gap is larger for the thin layers of GaSe. When the next layer is added to the particle, the band gap becomes smaller. As a limit, its value approaches 2.1 eV in the case of a thick macroscopic crystal.

IV. DISCUSSION AND CONCLUSIONS

The interlayer interactions in GaSe crystals, as in many other layered materials, are much weaker than the bonds inside tetralayers. Due to that, the ultrasonic treatment of the sample disrupts mostly the interlayer connections. The resulting material contains the thin GaSe platelets of different diameter. Their thickness can be reduced down to a single tetralayer. If the process of platelet agglomeration is suppressed (for instance, due to surfactants), one can sort out the fraction of crystallites with a reduced number of layers. This approach has been successfully realized for graphite. The fractions of graphene monolayers have been obtained.³⁰

The TEM images (Fig. 7) illustrate that sample B represents mostly the flat GaSe particles. Their thickness is estimated from one to a few tetralayers. The UV bands, arising in the optical-absorption spectra, should be due to a presence of these thin platelets.

The calculations in the Secs. II B and II C predict that the electronic structure of GaSe is strongly dependent on the number of layers that formed the crystal. According to the

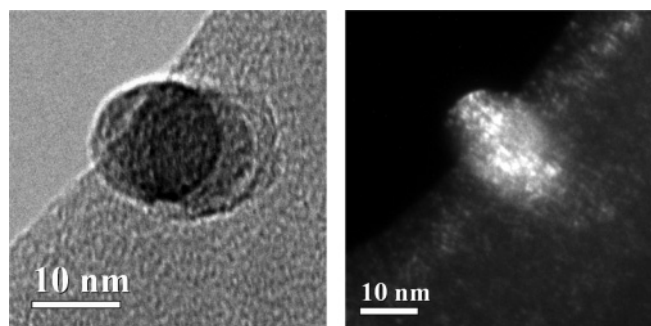


FIG. 8. A BF-TEM image of gallium selenide nanocrystals (left-hand side) and a DF-TEM image obtained in the (010) reflex zone axis [001] (right-hand side).

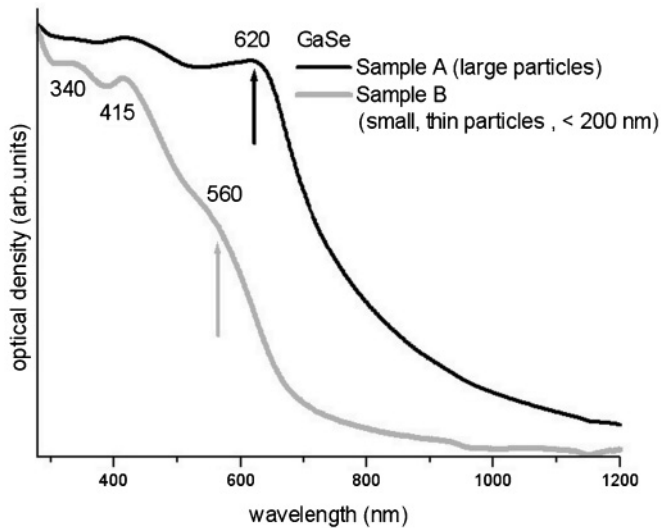


FIG. 9. The optical-absorption spectra of sample A (large particles of GaSe, suspended in water in the presence of the surfactant Pluronic F127) and sample B (small thin particles of GaSe, suspended in water in the presence of the surfactant Pluronic F127).

experimental data (Ref. 21), the absorption bands of the single tetralayer nanoparticles of GaSe are situated at 360–450 nm, and the center of the absorption shoulder at 400 nm was observed for nanoparticles with a large diameter (9 nm). For these nanoparticles, the radial quantum confinement effect should be almost negligible, and their absorption spectra would be similar to those of a single tetralayer sheet. The observed absorption UV band at 400–500 nm with a maximum at 415 nm can be attributed to the contribution of thin platelets with a thickness of one tetralayer.

If one assumes to have a mixture of GaSe crystals of various thicknesses (from a single tetralayer up to a few tetralayers), the resulting optical-absorption spectra should be a superposition of the transitions in all GaSe crystals (including the single, double, triple, etc., tetralayers). The wide band at 2.6–1.9 eV corresponds to multitetralayers, whose transitions are overlapped.

The calculated difference between the band gap of a single tetralayer and bulk GaSe is 1.55 eV (Fig. 5). The experimental onset of the absorption shoulder of GaSe single tetralayers is ~ 480 nm both for our data (Fig. 9) and in Ref. 25. The value observed experimentally is lower (~ 1 eV, Fig. 9). There is some difference between the calculated and experimental results. Even slight changes in the interatomic distances can significantly influence the electronic structure. The equilibrium geometrical parameters, obtained from the lattice optimization procedure, may differ from the experimental values. At the same time, lattice optimization has to be performed, since the experimental lattice parameters vary in a wide range for the bulk structure and are unknown for a single tetralayer structure. The temperature can be another reason for the discrepancy.

In conclusion, the electronic band structures of single, double, triple, and quadruple tetralayers of GaSe have been calculated. It has been revealed that the thickness of the crystal has a strong influence on its electronic structure. The two-dimensional thin GaSe crystals have a larger band gap than the bulk GaSe. The thin GaSe platelets were obtained experimentally. The absorption spectra of the sample, containing crystals with a thickness from a single to multiple tetralayers, demonstrate the UV bands, assigned to a single GaSe tetralayer.

The bulk GaSe crystals are indirect semiconductors. The energy difference between the direct transition at the Γ point and the indirect transition Γ - M is quite subtle. However, for a single, double, etc., tetralayers it may cause more sufficient changes. Both in theoretical and experimental results, the blueshift of the band gap is clearly seen.

ACKNOWLEDGMENTS

This work is supported by the RFBR-09-02-91231-CT_a and TUBITAK 108T587 projects, the federal target program Scientific and Pedagogic Personnel of Innovative Russia 2009–2013, Contract No. P1286, Russian President Grant No. MK-2164.2011.2, and the RAS research program “New materials.”

*rybkovskiyd@gmail.com

¹K. Maschke and F. Levy, in *Crystal and Solid State Physics*, edited by S. Flügge, Landolt-Börnstein, New Series, Group III (Springer-Verlag, Berlin, 1983), Vol. 17.

²A. Kuhn, A. Chevy, and R. Chevalier, *Phys. Status Solidi A* **31**, 469 (1975).

³F. Bassani and G. P. Parravicini, *Nuovo Cimento B* **50**, 95 (1967).

⁴H. Kamimura and K. Nakao, *J. Phys. Soc. Jpn.* **24**, 1313 (1968).

⁵J. McCanny and R. Murray, *J. Phys. C* **10**, 1211 (1968).

⁶E. Doni, R. Girlanda, V. Grasso, A. Balzarotti, and M. Piancentini, *Nuovo Cimento Soc. Ital. Fis., B* **51**, 154 (1979).

⁷S. Nagel, A. Baldereschi, and K. Maschke, *J. Phys. C* **12**, 1625 (1979).

⁸M. Schluter, *Nuovo Cimento B* **13**, 313 (1973).

⁹M. Schluter and M. Cohen, *Phys. Rev. B* **14**, 123 (1976).

¹⁰A. Bourdon, *J. Phys. (Paris), Colloq.* **C3**, 261 (1974).

¹¹M. O. D. Camara, A. Mauger, and I. Devos, *Phys. Rev. B* **65**, 125206 (2002).

¹²L. Plucinski, R. L. Johnson, B. J. Kowalski, K. Kopalko, B. A. Orłowski, Z. D. Kovalyuk, and G. V. Lashkarev, *Phys. Rev. B* **68**, 125304 (2003).

¹³V. N. Brudnyi, A. Kosobutsky, and S. Sarkisov, *Semiconductors* **44**, 1158 (2010).

¹⁴D.-W. Zhang, F.-T. Jin, and J.-M. Yuan, *Chin. Phys. Lett.* **23**, 1876 (2006).

¹⁵A. C. Ferrari, J. C. Meyer, V. Scardaci, C. Casiraghi, M. Lazzeri, F. Mauri, S. Piscanec, D. Jiang, K. S. Novoselov, S. Roth, and A. K. Geim, *Phys. Rev. Lett.* **97**, 187401 (2006).

- ¹⁶S. L. Stoll, E. Gillan, and A. Barron, *Chem. Vap. Deposition* **2**, 182 (1996).
- ¹⁷K. Allakhverdiev, J. Hagen, and Z. Salaeva, *Phys. Status Solidi A* **163**, 121 (1997).
- ¹⁸V. Chikan and D. F. Kelley, *Nano Lett.* **2**, 141 (2002).
- ¹⁹H. Tu, S. Yang, V. Chikan, and D. F. Kelley, *J. Phys. Chem. B* **108**, 4701 (2004).
- ²⁰H. Mirafzal and D. F. Kelley, *J. Phys. Chem. C* **113**, 7139 (2009).
- ²¹H. Tu, V. Chikan, and D. F. Kelley, *J. Phys. Chem. B* **107**, 10389 (2003).
- ²²X. Gonze, B. Amadon, P.-M. Anglade, J.-M. Beuken, F. Bottin, P. Boulanger, F. Bruneval, D. Caliste, R. Caracas, M. Cote, T. Deutsch, L. Genovese, P. Ghosez, M. Giantomassi, S. Goedecker, D. Hamann, P. Hermet, F. Jollet, G. Jomard, S. Leroux, M. Mancini, S. Mazevet, M. Oliveira, G. Onida, Y. Pouillon, T. Rangel, G.-M. Rignanese, D. Sangalli, R. Shaltaf, M. Torrent, M. Verstraete, G. Zerah, and J. Zwanziger, *Comput. Phys. Commun.* **180**, 2582 (2009).
- ²³X. Gonze, G.-M. Rignanese, M. Verstraete, J.-M. Beuken, Y. Pouillon, R. Caracas, F. Jollet, M. Torrent, G. Zerah, M. Mikami, P. Ghosez, M. Veithen, J.-Y. Raty, V. Olevano, F. Bruneval, L. Reining, R. Godby, G. Onida, D. Hamann, and D. Allan, *Z. Kristallogr.* **220**, 558 (2005).
- ²⁴K. Cenozal, L. Louise, M. Gelato, M. Penzo, and E. Parthe, *Acta Crystallogr., Sect. B: Struct. Crystallogr. Cryst. Chem.* **47**, 433 (1991).
- ²⁵H. Tu, K. Mogyrosi, and D. F. Kelley, *Phys. Rev. B* **72**, 205306 (2005).
- ²⁶L. Hedin, *Phys. Rev. A* **139**, 796 (1965).
- ²⁷M. S. Hybertsen and S. G. Louie, *Phys. Rev. Lett.* **55**, 1418 (1985).
- ²⁸E. Aulich, J. Brebner, and E. Mooser, *Phys. Status Solidi B* **31**, 129 (1969).
- ²⁹K. Allakhverdiev, M. Yetis, S. Özbek, T. Baykara, and E. Salaev, *Laser Phys.* **19**, 1092 (2009).
- ³⁰A. Green and M. C. Hersam, *Nano Lett.* **9**, 4031 (2009).